A Reactive Molecular Dynamics Study of Hygrothermal Degradation of Crosslinked Epoxy Polymers

Anas Karuth¹, Amirhadi Alesadi² Aniruddh Vashisth³, Wenjie Xia^{2*}, Bakhtiyor Rasulev^{1*}

¹Department of Coatings and Polymeric Materials, North Dakota State University, Fargo, ND 58108, United States

²Department of Civil, Construction and Environmental Engineering, North Dakota State
University, Fargo, ND 58108, United States

³Department of Mechanical Engineering, University of Washington, Seattle, WA 98195, United States

*To whom correspondence should be addressed, E-mail:

bakhtiyor.rasulev@ndsu.edu

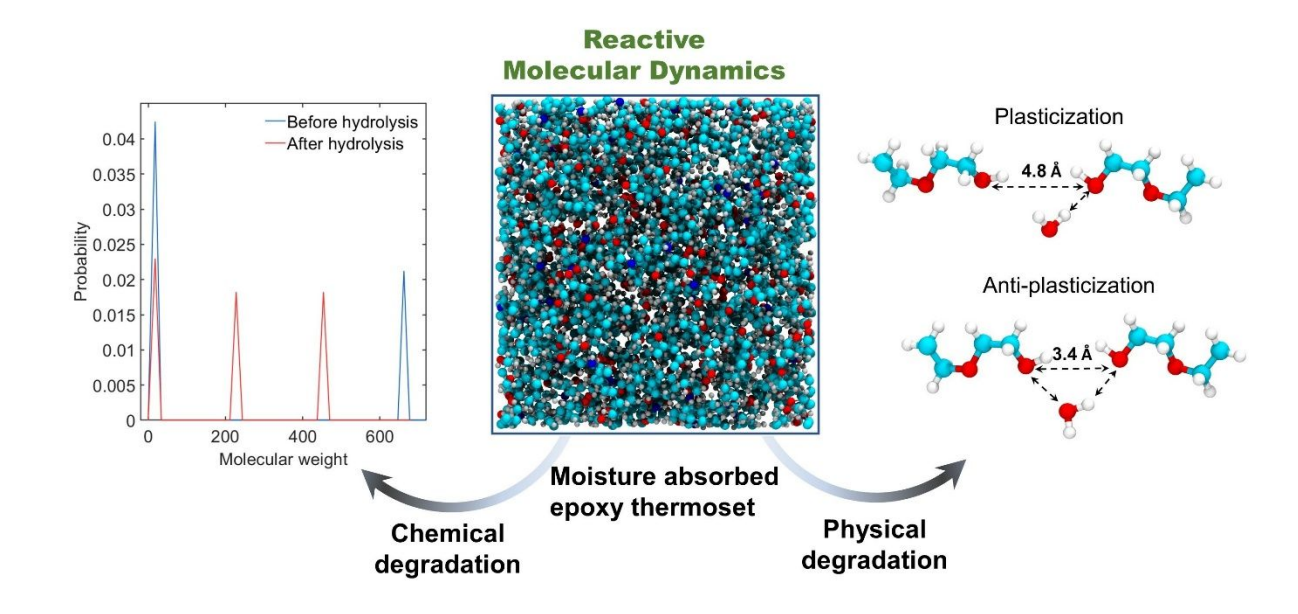
wenjie.xia@ndsu.edu

ABSTRACT

Epoxy thermosets are often exposed to high humidity environments in various applications, undergoing reversible and irreversible degradation depending on the environment. This study presents a reactive molecular dynamics (MD) simulation framework to gain deeper insights into the hygrothermal aging process, which is essential to develop a targeted approach to combat water assisted degradation in epoxy thermosets. By applying ReaxFF potential, an epoxy–amine network is created at low temperatures to avoid unwanted high temperature side reactions, where the water molecules are added to achieve the desired degree of moisture contamination. The simulations show that in addition to the plasticization effect from the moisture ingress, the epoxy network shows recovery in mechanical properties and density due to multi-site interaction of the water molecule with the electronegative sites within the network. Moreover, long term exposure to humidity or direct exposure due to cracking can induce irreversible changes in the epoxy-amine network. The protonation of the water molecule and nucleophilic attack on the C-O bond of the ether linkages in the epoxy-amine networks is successfully simulated by applying reactive MD simulations. Remarkably, the simulations show that the selectivity of water molecules for hydrolysis reaction in the epoxy network depends on the spatial arrangement and the steric hindrance of the network. This work provides molecular level insights into hygrothermal aging by elucidating the interplay between free volume and polarity of the network in the physical aging of the moist epoxy networks, paving a way for advanced design strategy towards better durability and performance of epoxy thermosets in humid environments.

Keywords: Hygrothermal degradation, Reactive molecular dynamics, ReaxFF, Epoxy-amine network, Polymers, Water absorption

TABLE OF CONTENT FIGURE



1. Introduction

Epoxy thermoset exhibits excellent thermal and mechanical properties, good adhesion, and resistance to chemicals, as well as anti-corrosion and better electrical insulation properties.¹ Various engineering and technological fields such as aerospace, marine, coatings, adhesives, electronic packaging, construction^{2–5} exploit the excellent performance and characteristics of epoxy thermosets. For many of these applications, epoxy polymers are often exposed to high humidity environments. The water absorption of epoxy thermoset would typically lead to the deterioration of its physical and mechanical properties. Moisture absorption in polymeric thermoset obeys Fick's second law of diffusion,⁶ and the water sensitivity of epoxy thermoset can induce reversible and irreversible changes in the crosslinked network.⁷ The affinity of epoxy thermoset with water is associated with polar hydroxyl groups formed during ring-opening polymerization of epoxide groups, 8 stoichiometric ratio of resin and hardner, 9 and the presence of other components. 10 Besides irreversible processes like hydrolysis 11 and photodegradation, 12 epoxy thermoset often undergoes physical degradation with water uptake inducing swelling, ¹³ deterioration in elastic and fracture properties, 14 loss of adhesion in the interface, 15 crack propagation, ¹⁶ and depression in its glass transition temperature. ¹⁷ The underlying chemical and physical degradation mechanisms in epoxy thermosets due to water ingression have been studied experimentally. 18-21 Despite the abundance of experimental studies on moisture ingress in epoxy thermosets, the molecular-level mechanism of physical and chemical degradation and associated nanoscale dynamics and dynamic evolution of hydrogen bonding in the network is still largely elusive.

To overcome these challenges, molecular dynamics (MD) simulation and other computational techniques^{22–32} are often used to offer molecular-level insights to physical and chemical

degradation mechanisms in the crosslinked epoxy polymers. Numerous MD simulations about the diffusion behavior of water molecules in epoxy thermoset and the resulting changes in the structure and properties have been reported. 14,33-36 Most of these MD simulations focused on calculating the diffusion coefficient and spatial distribution of water molecules in the epoxy network. Zhou and Lucas³⁷ proposed the existence of water in a free and bound state with hydrophilic groups in the crosslinked epoxy network and identified two types of bound water (TYPE I and TYPE II) using solid-state nuclear magnetic resonance (NMR) spectroscopy. Single site or multi-site interaction of water molecules with polar sites of the network differentiates TYPE I and TYPE II bonds. Only a few studies of MD simulations^{37-38,14} are devoted to understanding the dynamic evolution of bound water types (TYPE I and TYPE II) and their impact on the physical properties of epoxy networks. The type and quantity of hydrogen bonds formed between water and epoxy network depend on the polarity and free volume available in the network. An increase in the free volume of the network promotes TYPE I hydrogen bonds, and increased network polarity aids in the formation of TYPE II hydrogen bonds.³⁸ In a moist epoxy thermoset, TYPE I bonds facilitate plasticization, and TYPE II bonds are responsible for anti-plasticization. Plasticization in a crosslinked epoxy network often deteriorates thermal and mechanical properties.^{39,40} However, few investigations have reported the recovery in mechanical and thermal properties in epoxy thermosets at a certain amount of water content.^{33,34} T. Cui et al.¹⁴ has proposed that the plasticization effect is due to volumetric swelling of the network, and decreases the elastic modulus and fracture strain. They have shown that the anti-plasticization effect in the network generates partial recovery of elastic modulus. However, the nature and types of TYPE II bonds formed with epoxy networks during MD simulation have not been explored.

Atomistic MD simulation methods can be successfully used to analyze and evaluate the different types of TYPE I and TYPE II interactions in the moist epoxy thermosets. It is noteworthy that the water absorption in the epoxy-amine network depends on crosslink conversion, molecular weight distribution, the presence of unreacted epoxy and amine monomeric units, and other complex products. The realistic network formation with high crosslink density is important for the proper investigation of physical degradation in the moist epoxy network. It is impossible to experimentally achieve high crosslink density in epoxy thermosets due to diffusion limitation of monomers to the reactive sites after vitrification. To overcome these challenges, Vashisth et al. 42,43 proposed an Accelerated Reactive Force Field (ReaxFF) framework, which takes into account the reaction barrier energy, distances, and orientation reactant molecules. Once the reactant molecule satisfies the spatial configuration, the extra potential is provided to stretch and compress the bonds at a predefined rate to overcome the barrier energy of the epoxy-amine crosslinking reaction. The Accelerated ReaxFF can build an epoxy network with high-crosslink conversion and forms a network with the features of an experimentally formed epoxy thermoset.

On the other hand, the irreversible degradation or chemical modification of the epoxy thermoset system due to water absorption has gained little attention. The non-reactive force fields are inadequate in describing the reactive events during the simulation; this limitation has been resolved by the inclusion of connection-dependent terms in the non-reactive force field resulting in a reactive force field, ReaxFF. ReaxFF has been successfully applied to simulate many reactive degradation events, such as combustion reactions,⁴⁴ thermal decomposition⁴⁵ and biodegradation of polymers,⁴⁶ and metal-water reactions.⁴⁷ The incorporation of connectivity terms in the forcefield enables the study of the hygrothermal degradation in the epoxy thermoset. The ether linkages in the epoxy thermoset are susceptible to hydrolysis reaction. However, the neutral

hydrolysis of ether linkage is rare due to chemical stability. The hydrolysis of ether groups to alcohol is induced by a nucleophilic attack on the C-O bond of ether linkages. 48 The ab initio calculations have shown that the energy barrier for acid hydrolysis of dimethyl ether (DME) is ~40.0 kcal/mol and can vary depending on catalyst, solvent, size, and configuration.⁴⁹ The neutral hydrolysis study has been conducted using Accelerated ReaxFF on DME shows activation energy of 49.0 kcal/mol. 46 The ReaxFF framework provides extra energy to overcome the reaction barrier energy thereby initiating the hydrolysis and other reactions in the epoxy thermosets. Therefore, a knowledge gap exists in the comprehensive understanding of reversible and irreversible degradation mechanisms due to water ingress in the epoxy-amine system. This gap can be filled by using a reactive potential that can simulate the bond breaking and formation process using bond order formalism. Previous reported studies on physical and chemical degradation processes of the epoxy-amine system are dedicated to a single type of resin-hardener, which limits the investigation on the chemical structure or the variable nature of epoxy-hardener on the hygrothermal aging process. In this study, this gap has been addressed by comparing the hygrothermal degradation in two different types of epoxy thermoset. The epoxy resin used here is diglycidyl ether bisphenol-A (Bis A), which can be crosslinked with aliphatic (JEFFAMINE D-230) and aromatic amine (DETDA) curing agent, forming two different epoxy systems: 1) Bis A - JEFFAMINE D-230 and 2) Bis A - DETDA (Figure 1).

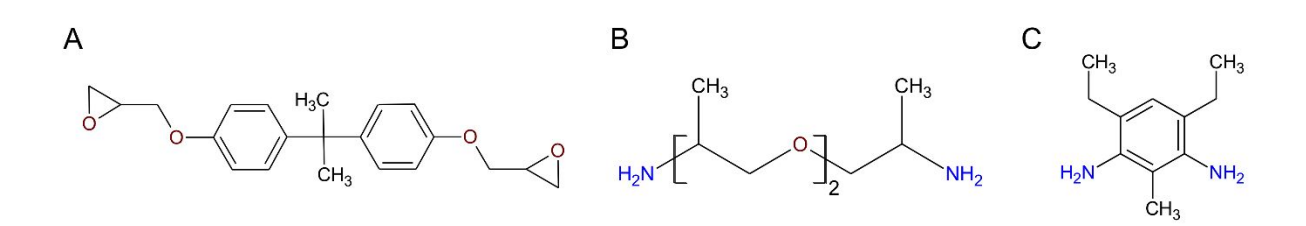


Figure 1. Structures of chemicals used for polymerization of epoxy-amine network: (A) Bisphenol

A diglycidyl ether (Bis A); **(B)** Polyetheramine (JEFFAMINE D-230), **(C)** Diethyltoluenediamine (DETDA).

In this work the Accelerated ReaxFF applied to study the physical and chemical degradation of two different epoxy-amine systems due to water absorption. First, the epoxy-amine crosslinked network is created using the ReaxFF framework. Both highly crosslinked epoxy-amine thermosets were absorbed with water at five different concentrations, i.e., 1, 2, 3, 4, and 5 wt %. First, we analyzed the moisture contaminated crosslinked networks of both epoxy-amine systems for physical degradation by subjecting them to mechanical deformation. The transportation characteristics of water in both crosslinked epoxy networks are estimated using MD. In addition, we explored and compared the spatial distribution and clustering behavior of water molecules in both systems. The inclusion of connectivity-dependent terms in the non-reactive force field enables us to investigate the hydrolysis reaction and hygrothermal aging in Bis A - JEFFAMINE D-230 and Bis A - DETDA systems. Importantly, understanding the moisture-induced physical and chemical degradation process in crosslinked epoxy polymers can advance the knowledge in mechanism of the moisture effect, paving the way for future materials-by-design strategies for tailor-made performance and durability.

2. METHODS

2.1 Overview of Reactive MD Simulation

The MD simulations are performed with the aid of the ReaxFF technique which utilizes the bond order formalism to describe reactive events.⁵⁰ The bond order is calculated from interatomic distances updated at every geometry optimization or time step of MD integration. This technique

provides a smooth transition between the nonbonded states and single, double, or triple bonded states, enabling the simulation of bond formation and breaking during chemical reactions for diverse materials. The energy contribution to ReaxFF potential is expressed as follows:

$$E_{system} = E_{bond} + E_{over} + E_{under} + E_{val} + E_{angle} + E_{tors} + E_{vdWaals} + E_{coloumb} + E_{lp} + E_{H-bond} + E_{rest}$$
(1)

The total energy of the system is inclusive of both bonded and nonbonded interactions. E_{bond} describes the energy required to form a bond between atoms, whereas over coordination (E_{over}) and under coordination (E_{over}) are listed as bond order and connectivity dependent terms. Energy penalty terms like E_{val} (valence angle energy), E_{tors} (torsion angle energy), and E_{lp} (lone pair energy) are also included in the total energy of the system. $E_{vdWaals}$ (van der Waals energy) and $E_{coloumb}$ (electrostatic energy) are nonbonded interactions calculated regardless of bond order and connectivity. The restrain energy E_{rest} is external energy added to desired atom pairs to drive a specific reaction. The summation of restrain energy to various pairs of an atom gives total restrain energy. Restrain energy is given as:

$$E_{rest} = F_1 \left(1 - e^{-F_2 (R_{ij} - R_{12})^2} \right) \tag{2}$$

 E_{rest} is restrain energy between two atom pairs in kcal/mol. F_1 and F_2 are force constant parameters for restrain energy having units kcal/mol and Å $^{-2}$, respectively. R_{12} and R_{ij} are target distance and the actual distance between the desired pair of atoms in the Å unit. The correct selection of the restrain parameters is critically important for driving the reaction between the epoxy resin and amine crosslinker to form epoxy thermoset and simulate the hydrolytic degradation of epoxy thermoset due to the interaction with absorbed water. The dispersion corrected force field dispersion/CHONSSi-lg,ff is utilized to drive the ring-opening of the epoxide

group and nucleophilic amine nitrogen attack on the tertiary carbon atom of the epoxide group. This dispersion corrected reactive force field (ReaxFF-lg) is developed to improve the long-range dispersion to obtain the correct density for molecular crystals and high energetic materials.⁵¹ The ReaxFF-lg has bonded, nonbonded, and long-range dispersion correction terms. However, the ReaxFF-lg is not effective for simulating the water interaction with condensed phases. To model the physical interaction and chemical modification of epoxy thermoset due to the water ingression, the *CHON-2017_weak* force field⁵² is applied. This force field improves the description of functionalized hydrocarbon/water weak interactions in the condensed phase. The details of both force fields and force constants used to drive the epoxy-amine crosslinking reaction can be found in the supporting information (SI) file.

2.2 Simulation of Crosslinking Procedure

Our research utilized the Amsterdam Density Function (ADF 2019.305) program⁵³ to simulate the epoxy - amine crosslinking reaction. The PLAMS (Python Library for Automating Molecular Simulation) tools in the ADF program provide a powerful, flexible, and easily extendable python interface to molecular modeling programs.⁵⁴ The epoxy-amine crosslinking reaction workflow using python script in PLAMS consisted of the following three steps: 1) Packing the reactants in the simulation box; 2) Accelerated crosslinking using bond boosting method; 3) Estimating the crosslinking ratio. More details of each step are shown in the supporting information (see section S2 in SI).

2.3 Water Absorption in Epoxy Thermoset

Water molecules were randomly inserted in the epoxy network formed by Accelerated ReaxFF. Five crosslinked epoxy-water models from both Bis A - JEFFAMINE D-230 and Bis A - DETDA systems were built by inserting 20, 40, 60, 80, 100 water molecules in the epoxy thermoset, which

correspond to 1, 2, 3, 4 and 5 wt% shown in **Figure 2**. The red spots in the epoxy network (wireframe model) are water molecules inserted in the interstices of the epoxy network.

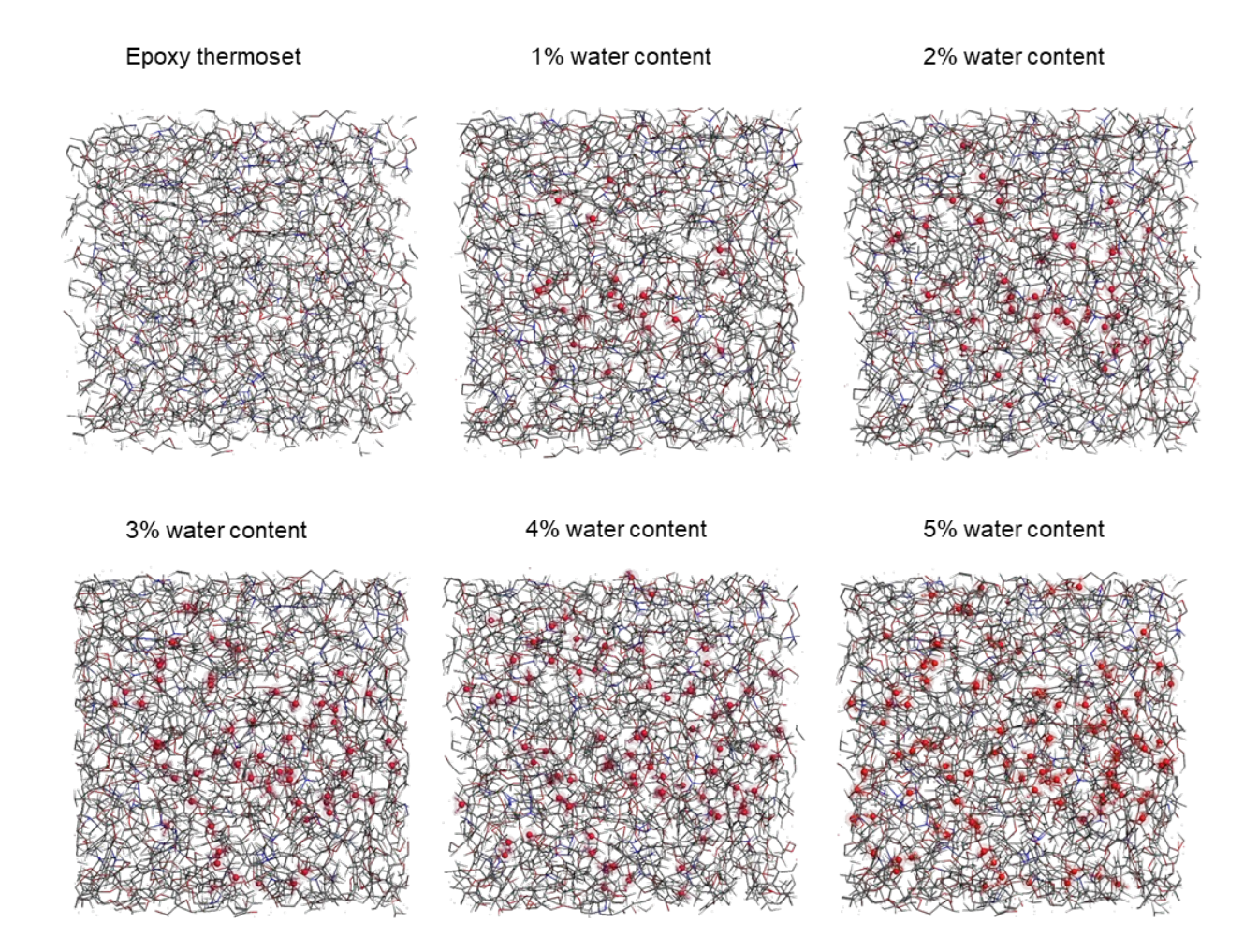


Figure 2. MD models of crosslinked epoxy-amine network with varying water content -wireframe model represents crosslinked epoxy-amine network and red spheres represent water molecules inserted in the interstices of the network.

The details of crosslinked epoxy-water MD models are illustrated in **Table 1**. This MD simulation will help to distinguish the effect of the chemical structure and density on physical and chemical degradation due to water absorption.

Table 1. Details of different MD models created for Bis A - JEFFAMINE D-230 and Bis A epoxy-DETDA systems.

Epoxy-amine thermoset	Number of water molecules	Number of atoms	Water weight (%)	Density (g/cm ³)
Bis A- JEFFAMINE D-230	0	5537	0	1.28
Bis A- JEFFAMINE D-230	20	5597	1	1.25
Bis A- JEFFAMINE D-230	40	5657	2	1.20
Bis A- JEFFAMINE D-230	60	5717	3	1.15
Bis A- JEFFAMINE D-230	80	5777	4	1.10
Bis A- JEFFAMINE D-230	100	5837	5	1.04
Bis A - DETDA	0	5369	0	1.19
Bis A - DETDA	20	5429	1	1.16
Bis A - DETDA	40	5489	2	1.08
Bis A - DETDA	60	5549	3	1.10
Bis A - DETDA	80	5609	4	1.01
Bis A - DETDA	100	5669	5	0.96

Water absorption results in volumetric swelling of epoxy thermoset and results in the rearrangement of molecular segments³⁶; To simulate this effect, the NPT dynamics simulation is carried out at 300 K and 0.1 MPa for 300 ps with 0.25 fs time step to equilibrate the system. The NPT dynamics decreases the density of the simulation box sharply and density starts to fluctuate about a well-defined mean point during the molecular dynamics time steps. This shows that the system attained an equilibrium density for a given temperature and pressure. The time-averaged density between 250 ps to 300 ps at five different water concentrations is reported in **Table 1**. The longer NPT dynamics (300 K and 0.1 MPa for 800 ps) was carried out to rule out the densification or dramatic evolution of the crosslinked system. The higher conversion ratio in epoxy- amine may have restricted further evolution of the system and attains equilibrium configuration in shorter time

period. The estimation of the equilibrium density of the water-epoxy thermoset model is illustrated in the SI (see section S3). The configuration with the density closest to the equilibrium value is used for further thermomechanical testing.

2.4 Property Calculations

Elastic properties of epoxy thermoset are calculated by applying tensile deformation in MD simulation. S5,56 Higher strain rates between 107/s to 1010/s are commonly employed in the MD simulation to compute the elastic modulus of epoxy thermoset in dynamic methods. S9,57 Strain rate of 2 x 108 s-1 is used in this study to deform the simulation box unilaterally with the constraint that the box shape remained cuboidal to calculate the elastic properties of the thermoset system. The faces of the cuboidal box parallel to the strain axis could approach each other due to the poison effect. The NPT Bredesen dynamics were carried out for 2 ns with a 0.25 fs time step at 300 K temperature and 0.1 MPa. The stress-strain response fluctuates due to the significant vibration of atoms on an atomistic scale. The elastic modulus is calculated from the slope of a linear fit to the small strain regime (< 0.05) in the stress-strain curve. The cuboidal box is strained in all three directions and the average value mechanical properties are reported.

The diffusibility of the water molecules can provide insights into the structure-property relationship of polymeric networks. The dynamics of water molecules in the epoxy thermoset were quantified by calculating the mean square displacement (MSD) of the water molecules in the network. It is a two-dimensional function defined as the square of the average distance that the water molecule has moved away from its starting point within the time interval τ as given by Equation (3). This function contains the diffusivity of observed molecules; the steeper they raise to higher values faster the observed particle diffusing in the system. The slope of the MSD will yield the diffusion coefficient of the observed particles as Equation (4)

$$MSD(\tau) = \left\langle |\overrightarrow{r_i}(t+\tau) - \overrightarrow{r_i}(t)|^2 \right\rangle \tag{3}$$

$$D(\tau) = \lim_{\tau \to \infty} \frac{1}{6\tau} \left(|\stackrel{\rightarrow}{r_i}(t+\tau) - \stackrel{\rightarrow}{r_i}(t)|^2 \right)$$
 (4)

For studying the MSD of water molecule in epoxy thermoset, firstly we carried out the NPT ensemble dynamics for a period of 500 ps with 0.25 fs time step at 600 K. The equilibrium density is estimated from the time-averaged densities (the last 200 ps out of all 500 ps). The configuration with the density closest to the equilibrium value was then used to initiate NVT ensemble dynamic for 600K for 2 ns with 0.25 fs time step.

The MSD of water molecules through the interstice of epoxy thermoset is evaluated using Trajectory Analyzer and Visualizer (TRAVIS).⁵⁸ The diffusion coefficient of water molecules is calculated by plotting a log (MSD) vs. log(t) plot, where the slope = 1 marks the true diffusive region. The estimation of the true diffusive region and diffusion coefficient is depicted in supporting information (see section S5). To speed up the kinetics of the diffusion and better statistical sampling, we simulate the epoxy-water models at elevated temperature.

2.5 Bond Boost Method for Accelerated Hydrolysis

Analogous to Accelerated ReaxFF for crosslinking, the hydrolysis reaction of epoxy thermoset can be simulated using the bond boost method. *CHON-2017_weak* force field is used to model the hydrolysis reaction of the crosslinked epoxy network. Respective atoms were tagged for boosting the hydrolysis reaction, once the distance criterion is satisfied, the extra potential is applied. The NVT simulations were performed to find the reaction energy barrier for the hydrolysis reaction using two water molecules and an amine-cured epoxy backbone. The reactive regions of the two water molecules and the amine cured epoxy backbone are highlighted and marked as shown in **Figure 3**. The force parameters reported for ether hydrolysis in the later work⁴⁶ are used to

investigate the hydrolysis reaction of the epoxy thermoset. These force parameters used for hydrolysis reaction of ether linkages which can correctly capture the reactive events as seen thorough QM calculations. The oligomer (Bis A – DETDA) selected for simple hydrolysis have only two ether linkages due to the formation of only primary amines. The formation of secondary amines in epoxy-amine reaction needs higher restrain energy due to spatial constraints and steric hindrance⁴². The force parameters for the hydrolysis of epoxy-amine thermoset are given in the SI, see section S1).

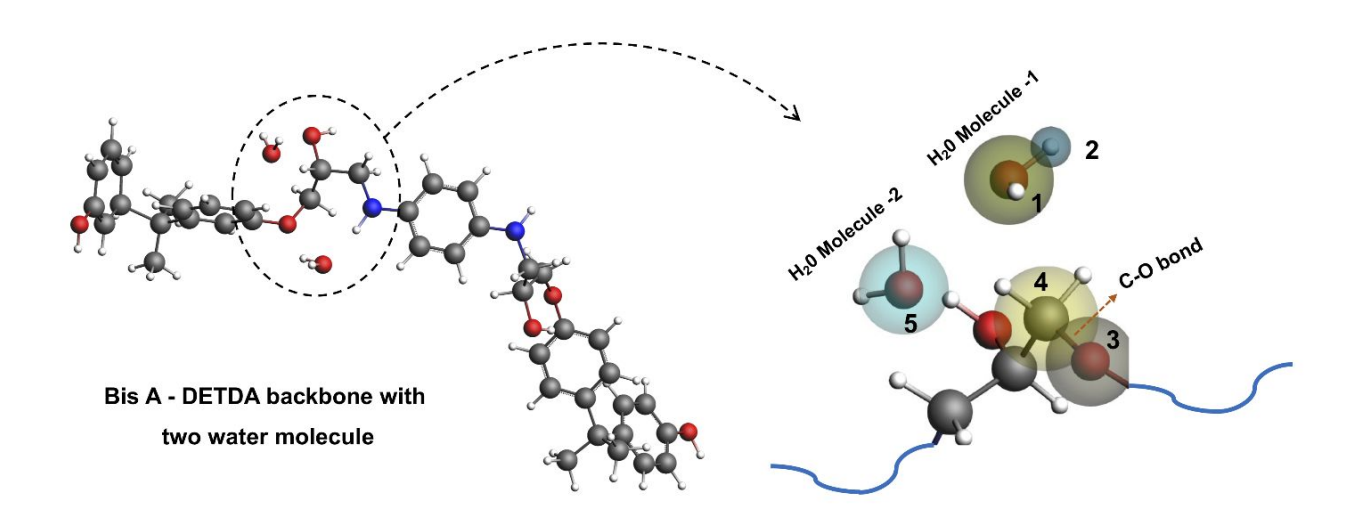


Figure 3. Assigning the regions for epoxy-amine thermoset backbone (Bis A - DETDA) and two water molecules for hydrolysis using the accelerated bond boosting method. The highlighted regions are O1 (oxygen atom of water molecule -1), H2 (hydrogen atom of water molecule -1), O3 (oxygen atom of ether linkages in epoxy - amine thermoset), C4 (carbon atom of ether linkages in epoxy - amine thermoset), and O5 (oxygen atom of water molecule -2).

Once the reactive barrier is estimated by simulating the simple hydrolysis reaction using two water molecules on the amine cured epoxy backbone, the same force parameters are used to study the bulk hydrolysis. To study the response of aromatic and aliphatic amine cured epoxy backbone to

hydrolysis reaction the bulk hydrolysis reaction is carried out for both epoxy thermosets. Both systems were inserted with 20 water molecules and non-reactive NVT simulation is carried out for the random distribution of water inside the interstices of the network. Subsequently a reactive NVT simulation at 500 K for 500 ps with a time step of 0.25 fs is performed using the same force constants obtained from simple hydrolysis.

3. RESULTS AND DISCUSSION

3.1 Epoxide-Amine Thermoset Formation. The non-catalyzed epoxide-amine crosslinking reaction was driven by the correct selection of force parameters F_1 , F_2 , and target distance R_{12} . This enabled us to calculate the approximate barrier energy for the crosslinking reaction. Vashisth et al.⁴² compared the different sets of force parameters for non-catalyzed, water-catalyzed, and self-promoted epoxy-amine crosslinking reactions and found a good agreement between ReaxFF and quantum mechanics (QM) energy barriers. As discussed previously in the bond boosting method (see in SI section S2), both crosslinking and compression of the cuboidal box are done simultaneously to adjust the density to a realistic density of 1.2 ± 0.05 g/cm³. The final molecular structure of Bis A - DETDA and Bis A - JEFFAMINE D-230 consists of 5369 and 5537 atoms, respectively. **Figure 4 (A)** shows the distance between the atom pairs (nitrogen atom 'N' of amine and terminal carbon atom 'C' of epoxide molecule) decreases during the simulation and achieves a fixed distance of 1.5 Å at 6 ps. This result indicates that extra potential applied in restrain energy overcomes the barrier energy to open up the epoxy ring and form an N-C covalent bond.

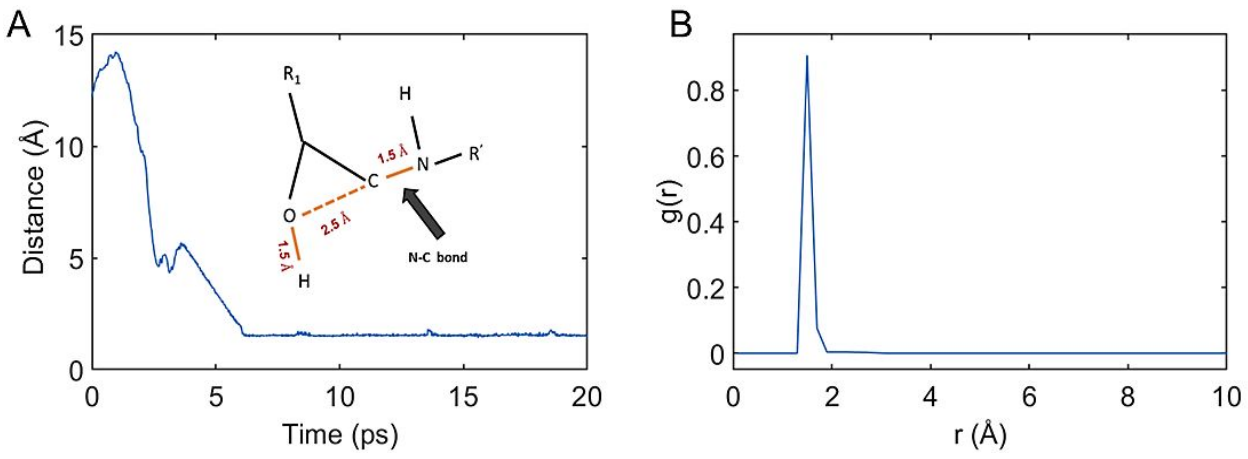


Figure 4. (A) Distance between the nitrogen atom (N) of amine and the terminal carbon atom (C) of Bisphenol A diglycidyl ether during MD steps; **(B)** Intermolecular radial distribution functions between nitrogen atoms of amine and the carbon atom of Bisphenol A diglycidyl ether. The

intermolecular radial distribution function (RDF) gives valuable insight into the structure of the system as it represents the probability of two atoms being at a specific distance from each other.

The presence of a sharp peak as shown in **Figure 4B** at 1.5 Å in the RDF of the pair of interest (N atom of amine and the terminal C atom of the epoxide molecule) indicates a covalent bond formation between N and C atoms. The final crosslink conversion for Bis A - JEFFAMINE D-230 and Bis A - DETDA is 70.5 % and 71% respectively, calculated by dividing the number of C-N bonds formed by the possible C-N bonds. The vitrification of the system restricts the unreacted monomers and small fragments to react with reactive sites of the growing chain due to diffusion limitation. ^{59,60} This has resulted in 40 ps more needed time for Bis A - JEFFAMINE D-230 system to reach the same conversion percentage of Bis A - DETDA systems. This difference in the time can be attributed to the diffusion limitation of JEFFAMINE D-230 to the reactive epoxy sites due to the longer aliphatic chain structure. The details of the final structure and crosslink conversion of both Bis A - JEFFAMINE D-230 and Bis A - DETDA can be found in the SI file (see section S2).

3.2 Physical Degradation in Thermosets. To study the physical degradation of epoxy thermosets, five different epoxy-water MD model was created for each epoxy-amine system (**Table 1**). The water molecules were inserted in the final structure of the epoxy-amine thermoset at varying concentrations of 1, 2, 3, 4, and 5 wt %. The MD simulations were carried out under NPT ensemble for 300 ps with 0.25 fs time step at 300K to attain the equilibrium density of the system. We observed that density decreases substantially within 100 ps, due to the increase in the simulation box volume. This increase in the box size is attributed to the interaction of water and epoxy networks, which led to subsequent swelling. The major density adjustment of the simulation box

happened within the first 100 ps and fluctuated around a well-defined mean point between 100 to 250 ps. The system attains an equilibrium density between 250 to 300 ps at a given temperature and pressure. The time-averaged density at this time scale range was reported as the final density of the epoxy-water MD model for both Bis A - JEFFAMINE D-230 and Bis A - DETDA at all water concentrations shown in **Table 1**. The density vs time plot of Bis A- DETDA system with 5 wt % of water content is shown in Figure S3 of SI. The final network structure for further thermomechanical testing and degradation study is selected from the equilibrium density region. This confirms that greater affinity of water with polar epoxy-amine network results in plasticization of the network due to volumetric swelling. The swelling of the network can increase the distance between the chains in the network, which results in lower intermolecular interactions. The impact on elastic modulus due to the swelling of the network is illustrated in **Figure 5A**. The Bis A - DETDA network has shown a decreasing trend in elastic modulus and density with the increasing water content. However, at 3 % water content, the elastic modulus and density of the Bis A - DETDA system exhibits a recovery trend. In the upcoming session, we will explore the molecular-level mechanism responsible for the recovery of elastic properties and density of the epoxy-amine network.

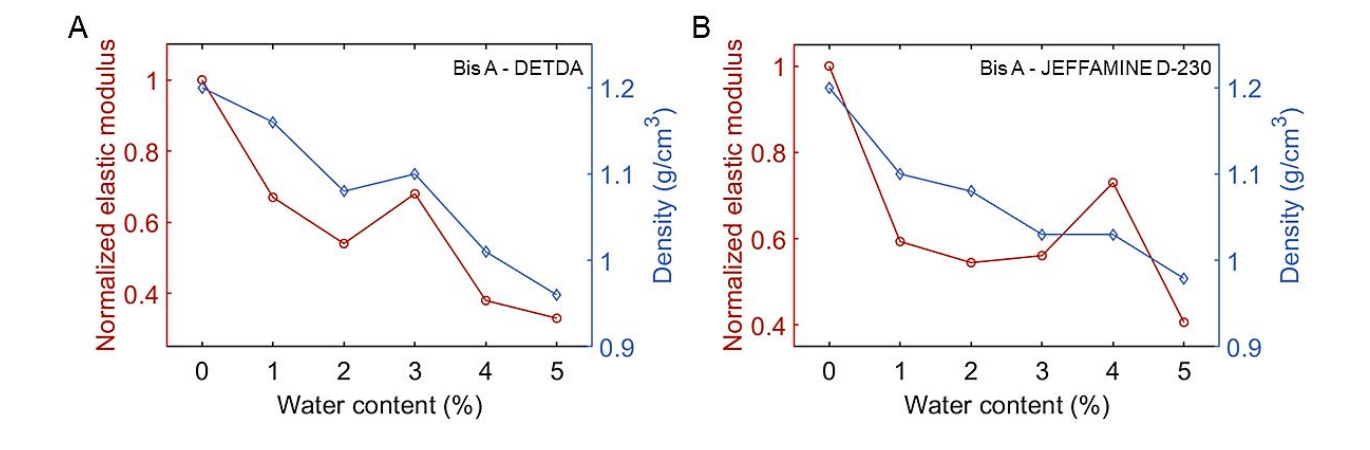


Figure 5. The normalized elastic modulus and density change in epoxy - amine thermoset with varying water content in **(A)** Bis A - DETDA and **(B)** Bis A-JEFFAMINE D-230.

As discussed previously, the bound water in the epoxy thermoset is classified as TYPE I and TYPE II, depending on their activation energy for desorption. The studies have shown that the desorption of bound water molecules expends energy between 5 to 20 kcal/mol.³⁷ This means that the water interacts with the epoxy network via hydrogen bonding mechanism, rather than physical interaction like Vander walls or dipole-diploe interactions.⁶¹ The activation energy difference for desorption in TYPE I and TYPE II hydrogen bonding is related to its ability to form single or multi-site hydrogen bonds with the network. Rishabh et al.³⁸ calculated the number of TYPE I and TYPE II hydrogen bonds in the epoxy - amine thermoset with different crosslinking conversions. They argued that the polarity of the system and free volume are two competing factors that determine the formation of one type of hydrogen bond over the other. Type II hydrogen bond formation is favored by the higher polarity of the network, and TYPE I hydrogen bond formation is favored by a larger free volume for a water molecule to form a cluster.

Figure 6A illustrates the dynamic evolution from TYPE I bond to the TYPE II hydrogen bond at 3% water content in the Bis A - DETDA system. The distance between the H atom of the hydroxyl group and O atom of water was tracked simultaneously with the distance between H atom of water with O atom of another neighboring hydroxyl group. We observed that the presence of TYPE I bond in the first 50 ps of MD simulation time scale, where the distance between the O atoms of the neighboring hydroxyl group is increased up to 4.8 Å. Above 75 ps the water molecule interacts with both hydroxyl groups in the epoxy network to form TYPE II hydrogen bonds. This multi-site interaction results in an anti-plasticizing effect and decreases the hydroxyl group distances from

4.8 Å to 3.4 Å. These increased intermolecular interactions promote the recovery of the elastic properties and density in the epoxy-amine system. The recovery in properties of moist epoxy-amine network depends on the rate of the dynamic evolution of TYPE I to the TYPE II hydrogen bond in the network. The moist network of Bis A - DETDA system with 3% water content provides a conducive environment for the faster transformation of the TYPE I to the TYPE II hydrogen bond. In other words, the rate of transformation of TYPE I to the TYPE II hydrogen bond in the network. The balance between the polarity and free volume of the network might have facilitated this transformation and thereby contributed to the recovery in the elastic properties and density.

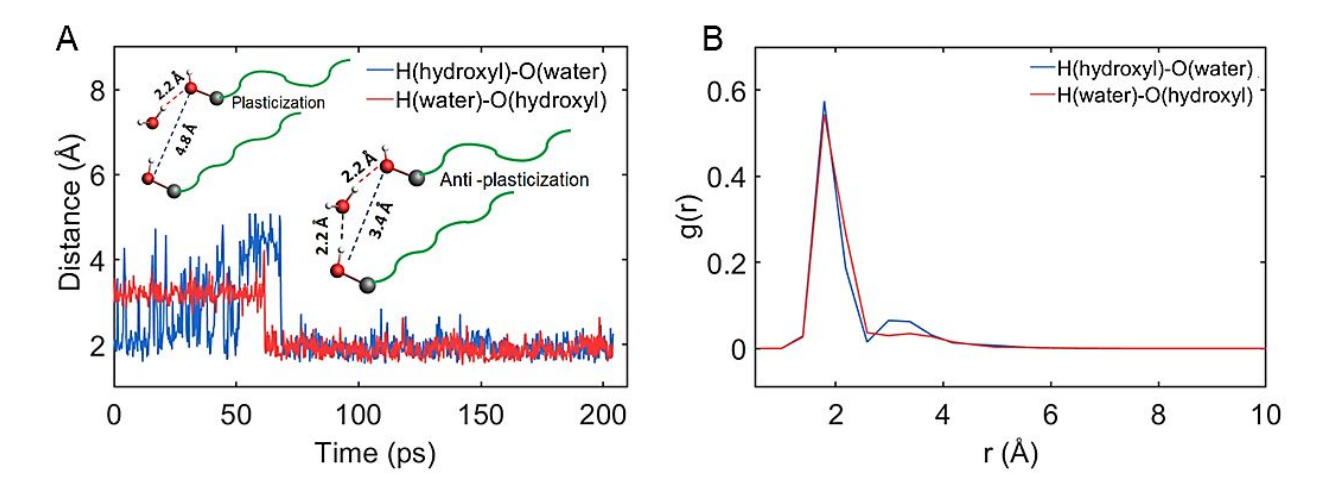


Figure 6. (A) Dynamic distance between a single water molecule and two hydroxyl groups (OH) of the Bis A - DETDA system during MD steps at 300K; **(B)** The probability distance distribution function of a given water molecule and two hydroxyl groups (OH) of the Bis A - DETDA system.

The sharp peak at 2.1 Å in the probability distance distribution function plot (**Figure 6B**) shows that the oxygen atom of water forms a strong hydrogen bond with the H atom of the hydroxyl group. Similarly, the H atom of the water molecule forms a hydrogen bond with the O atom of the

neighboring hydroxyl group at 2.1 Å. The water molecule bridges between two hydroxyl groups and acts as a secondary crosslinker. After all available hydrogen bonding sites in the epoxy network are saturated, further water ingression can decrease the elastic modulus and density of the network. In the Bis A - JEFFAMINE D-230 system, elastic modulus recovery happens at 4% water content, whereas the same happens at 3% for the Bis A - DETDA system. This difference in the water concentration on the elastic modulus recovery may have accounted for the chemical structure of the JEFFAMINE D-230 crosslinker. The long aliphatic amine crosslinker has two additional oxygen atoms in the monomeric unit, which contributes to more available hydrogen bonding sites and total polarity in the system. Thus, for saturating all available sites, more water content is needed in Bis A - JEFFAMINE D-230 system compared to the Bis A - DETDA system at the same crosslink conversion level. Like the Bis A - DETDA system, further water ingression can lead to a drastic decrease in elastic modulus and density in the Bis A - JEFFAMINE D-230 system. TYPE II hydrogen bonds are not restricted to only the hydroxyl groups in epoxy - amine, but can also form multi-site interaction with one hydroxyl group and H atom of the polymeric backbone. The details of this interaction are shown in supporting information (see section S4 in SI).

3.3 Diffusion and Spatial Distribution of Water Molecules in Thermosets. The study of diffusion of a water molecule in a polymeric network matrix provides useful information about the water and polymer interaction. **Figure 7A and B** illustrates the mean square displacement (MSD) of water in the Bis A - DETDA and Bis A - JEFFAMINE D-230 systems at varying water contents. The previous studies showed that the mobility of water molecules in epoxy thermosets increases with increasing water content and temperature. ⁶² The Bis A - JEFFAMINE D-230 system shows a lower MSD of water at all investigated water contents than the Bis A - DETDA system. The Bis A - JEFFAMINE D-230 system has a higher density (as seen in **Table 1**) at all corresponding

water content and higher polarity than the Bis A - DETDA system. The polarity of the network is classified by its ability to form strong and weak hydrogen bonds with water molecules.

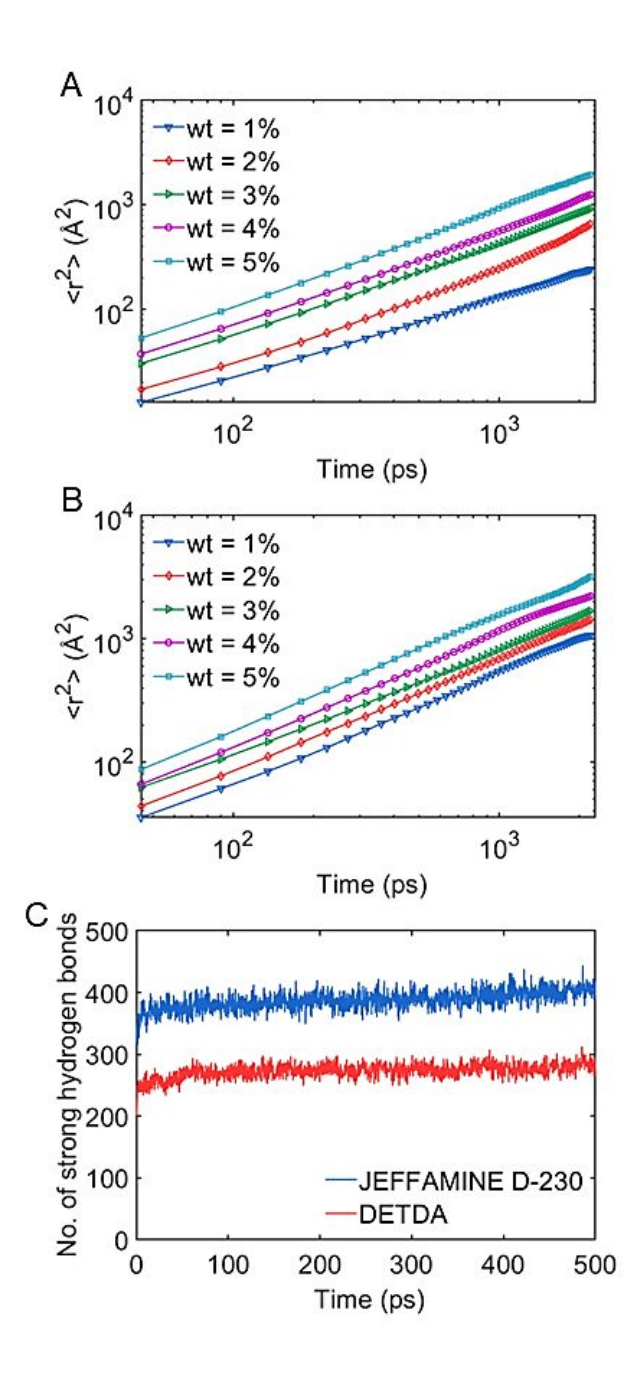


Figure 7. The mean square displacement of water in epoxy - amine thermoset at varying water content at 600K (A) Bis A - JEFFAMINE D-230 and (B) Bis A-DETDA. (C) The number of

strong hydrogen bonds formed during MD in Bis A - JEFFAMINE D-230 and Bis A - DETDA thermoset at 2 wt % water content.

Figure 7C shows the number of strong hydrogen bonds formed by both systems at the same water content of 2%. The range of hydrogen bond distance for strong and weak hydrogen bonding is observed to be about 2 - 3.2 Å and 3.3 - 4 Å, respectively.63 The Bis A - JEFFAMINE D-230 system forms more strong hydrogen bonds than the Bis A - DETDA system. This plot estimates the cumulative sum of hydrogen bonds formed in each system in MD steps due to interactions between epoxy thermoset and water. The chemical structure of the JEFFAMINE D-230 crosslinking agent facilitates more sites for hydrogen bonding than the DETDA crosslinker in the epoxy system. In other words, the increased polarity in Bis A - JEFFAMINE D -230 system results in a lower MSD of water than the Bis A - DETDA system. The synergy of lower free volume and higher polarity impedes the mobility of water. Sylvian et al.⁶⁴ proposed that when the interaction sites in the polymer are saturated with water, the absorption reaches quasi-equilibrium. Further incoming water is occupied in the microvoids to form a cluster and reaches equilibrium after filling all microvoids. Figures 8A and B illustrate the pair correlation function between oxygen atoms of a water molecule in both systems. This can elucidate the spatial distribution of water molecules in the network and their interaction with the network The intermolecular RDFs between oxygen atoms on water molecules at all concentrations show a sharp peak at 2.9 Å for both systems. This indicates the water molecules can form hydrogen bonds with each other, but the probability of forming a hydrogen bond at a distance of 2.9 Å decreases with the increased water concentration. This is in agreement with previous MD simulations reported on other polymeric systems, 65,66 as

well as for DGEBA epoxy cured with cyclic amines.³⁶ This is due to the ability of water molecules to cluster (collection of small aggregate) each other at high concentrations.

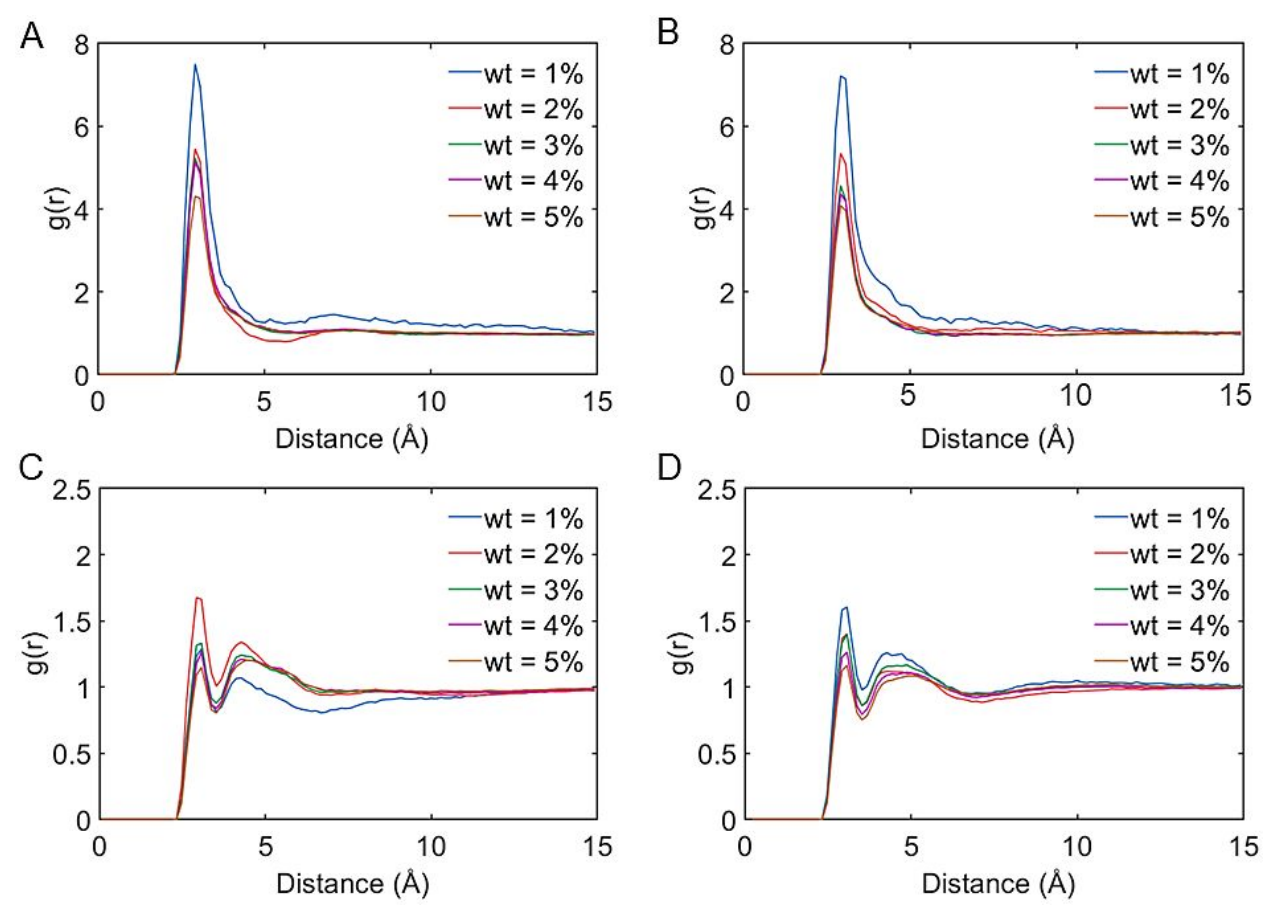


Figure 8 Intermolecular radial distribution functions between oxygen atoms of water molecules from NVT dynamics at 600K for 2 ns (A) Bis A - JEFFAMINE D-230 and (B) Bis A - DETDA systems with water concentration. Intermolecular radial distribution functions between polar atoms of epoxy network and water molecules from NVT dynamics at 600K for 2 ns (C) The Bis A - JEFFAMINE D-230 system and oxygen atoms in water molecules with varying water content. (D) The Bis A - DETDA system and oxygen atoms in water molecules with varying water content.

Figures 8C and **D** show the RDFs between a pair of oxygen atoms (oxygen atom in the water and oxygen atom in the polymer network) in five different moist networks of both systems. In the Bis

A - JEFFAMINE D-230 system, two different peaks at distances of 2.2 Å and 4.2 Å are shown at all water content levels. The sharp peak at 2.2 Å indicates the presence of a hydrogen bond between water and polar groups of backbone. The broad peak of 4.2 Å is associated with the symmetry of polar groups in the network. ²⁸ Similarly, in Bis A - DETDA system, we observed sharp and broad peaks at distances of 2.9 Å and 3.7 Å, respectively. In Bis A - JEFFAMINE D-230 system, the water tended to be located in the proximity of the polar group at an average interatomic distance of 2.2 Å, but Bis A - DETDA system water tends to be located at 2.9 Å. The difference in the hydrogen bonding distance of both systems can be related to the rigidity of the backbone. The previous MD study shows that the dynamic mobility of polymer chains facilitates the ingress pathway for moisture in the epoxy network.⁶⁷ The flexible backbone of the Bis A - JEFFAMINE D-230 system decreases the average hydrogen bond distance between polar groups and water compared to the rigid backbone in the Bis A - DETDA system. In both systems, the change in water content does not change the interatomic distance (peak position), but the peak height changes with water content. In Bis A - JEFFAMINE D-230 system (Figure 8C), we observed that the peak intensity at 2.2 Å (indicating the strength of forming hydrogen bond) has a non-monotonic trend. It first increases with water content, and after 2 wt% it reduces sharply. This can be due to the saturation of hydrogen bonding sites in the network with water; after saturation, the additional water tends to cluster around each other (as described in the previous section). In other words, 2% water content is required for this system to saturate with all accessible hydrogen bonding sites in the network. However, in the Bis A - DETDA system, 1% water content is required for saturation of all accessible polar sites in the network, and further addition of water forms clusters. This trend is visible in Figure 8D, as the increasing water content does not contribute to hydrogen bonds with

the network. It should be noted that the number of polar groups in each system for hydrogen bonding is constant at all levels of water content.

3.4 Chemical Degradation in Epoxide-Amine Thermosets. The long-term exposure of epoxy thermoset to water leads to irreversible (chemical) degradation. For example, several studies emphasize the chemical degradation of anhydride cured epoxy thermoset with water. 11,68–70 The neutral ester hydrolysis reaction using ab initio calculations and continuum solvation model was investigated using different mechanisms.⁷⁹ Unlike the ester linkages in anhydride cured epoxy thermoset, the amine cured epoxy thermoset has ether linkages in the backbone. A good agreement has been found between quantum mechanical (QM) and ReaxFF data for energy barrier for ester and ether hydrolysis.⁴⁶ The neutral hydrolysis of ether linkages in the epoxy thermoset is less favorable due to chemical stability. However, acid-catalyzed hydrolysis of dimethyl ether in the presence of water and hydronium ions was studied.⁴⁹ The neutral water acts as an acid and protonates oxygen, leaving a strong nucleophile.⁴⁸ The liberation of strong nucleophiles for the cleavage of ether linkage in epoxy-amine thermoset is a highly energetic process. To overcome this energy barrier for ether hydrolysis, high restrain energy is required in the ReaxFF framework. The average restrain energy for ester hydrolysis and ether hydrolysis were reported as 53 and 77 kcal/mol, respectively.⁴⁵

3.5 Simple Hydrolysis The elementary hydrolysis reaction of Bis A - JEFFAMINE D-230 and Bis A - DETDA were studied using two water molecules on the epoxy thermoset backbone. **Figure 9A** illustrates that the two water molecule approaches the ether linkages (C-O-C) to meet the spatial configuration for a steering hydrolysis reaction. Once the equilibrium configuration is satisfied, the extra potential was applied to stress and compress the C-O bond of the ether linkage. The water reacts with the carbon atom of the C-O bond to form a transition state structure as shown

in **Figure 9B**. The unstable transition state structures form desired products or revert to reactants depending on the success of the reaction. **Figure 9C** shows the successful hydrolysis reaction of the ether backbone to form two alcohols.

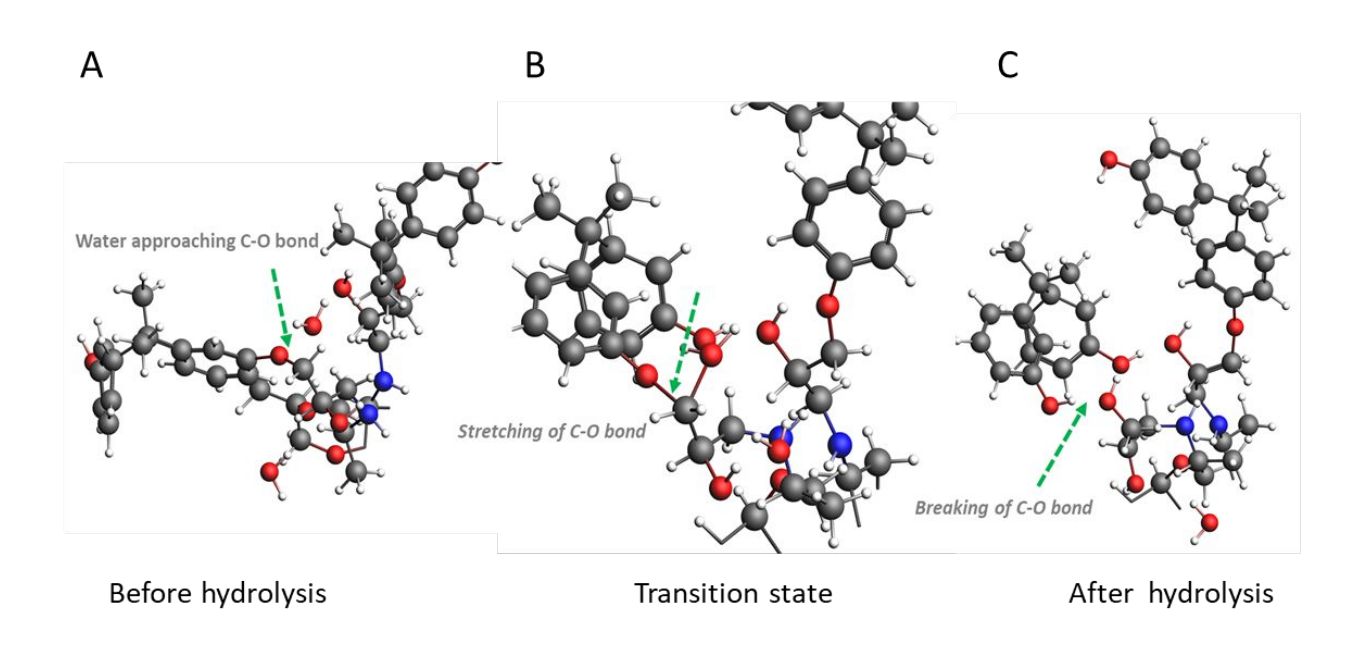


Figure 9. Snapshots of the elementary hydrolysis reaction of Bis A - DETDA: **(A)** Before hydrolysis, **(B)** Transition state, and **(C)** After hydrolysis.

It is evident from the restrain energy calculation that the spatial arrangement of atoms and steric hindrance plays an important role in the hydrolysis reaction of C-O bonds in ether. The energy barrier for hydrolysis reaction of Bis A - DETDA is higher than Bis A - JEFFAMINE D-230 system. The details of restrain energy for both systems can be found in the supporting information (see section S6). The aromatic amine crosslinking agent in Bis A - DETDA may provide higher steric hindrance and thereby reducing the rate of hydrolysis reaction with ether groups. The radial distribution function plot for the O atom of ether and the H atom of water, as

well as the C atom of ether and the O atom water in the Bis A - DETDA system, is shown in **Figure 10A**. The sharp peaks at 0.95 Å and 1.5 Å indicate O-H and C-O bond making by breaking ether linkages (C-O-C) in the Bis A - DETDA network. The O-H and C-O bond formations indicate the protanation of the oxygen atom and strong nucleophile attack on the ether linkages to form alcohol groups.

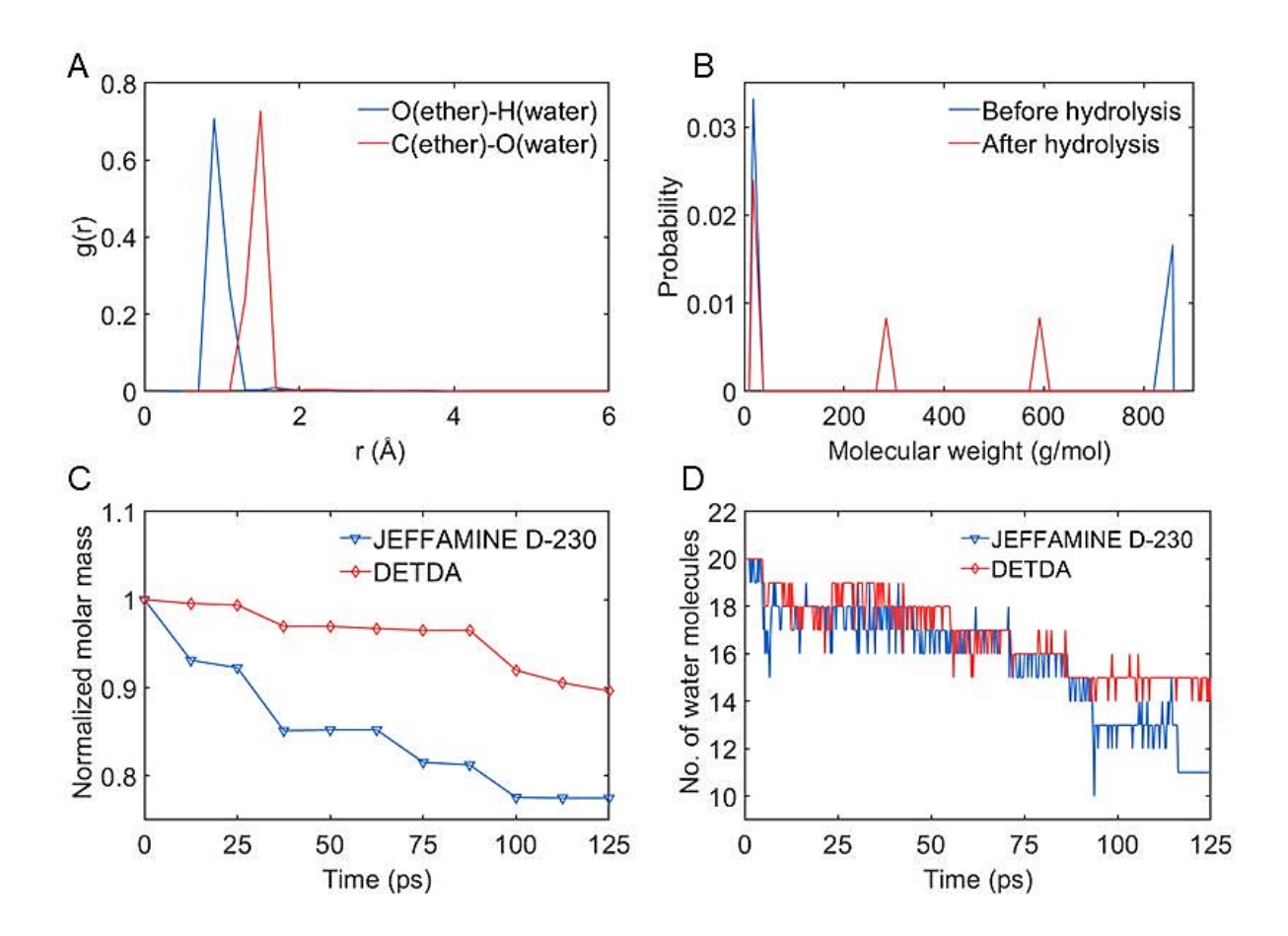


Figure 10. (A) The radial distribution function of O-H and C-O bond in Bis A - DETDA system. The molecular weight distribution of the Bis A - DETDA system **(B)** before hydrolysis and after hydrolysis. **(C)** The number of water molecules consumed during hydrolysis reaction of epoxyamine thermosets in MD simulation using ReaxFF. **(D)** The molecular weight reduction of the

largest fragments in epoxy - amine thermosets during the hydrolysis reaction in MD simulation using ReaxFF.

Figure 10B illustrates the molecular weight distribution before and after the ether hydrolysis in the Bis A - DETDA system. Before the hydrolysis reaction was triggered, the system has only two types of molecular weights, which correspond to 18 g/mol (water) and 859.5 g/mol (two Bis A molecules crosslinked with a DETDA crosslinker). Hydrolysis results in the fragmentation of crosslinked molecules to produce lower molecular weight fragments with molecular weights of 285.2 g/mol and 592.3 g/mol. The nucleophile-assisted hydrolysis of the C-O-C bond in ether is possible, due to the formation of strong nucleophiles from water dissociation. The participation of one water molecule in the hydrolysis reaction reduces the probability of water molecules' presence in the final products. The same pattern of hydrolysis is observed in the Bis A - JEFFAMINE D-230 system.

3.6 Bulk Hydrolysis. To understand the extent of hydrolysis in the Bis A - JEFFAMINE D-230 and Bis A - DETDA systems, we carry out the bulk simulation of the hydrolysis by inserting 20 water molecules inside both epoxy thermosets, as mentioned in the method section. The accelerated ReaxFF simulation for both the Bis A - JEFFAMINE D-230 and Bis A - DETDA systems were performed with the same force constants. **Figure 10D** shows the amount of water consumed during NVT dynamics at 500 K for 500 ps for a timestep of 0.25 fs in both systems. Initially, 20 water molecules are present inside both the aliphatic and aromatic amine cured epoxy thermoset. As the time proceeds in MD simulations, the number of water molecules decreases as they dissociate to form OH and H ions. This strong nucleophile (OH⁻) attack on the C-O bond of ether linkage results in the cleavage of C-O bonds to form alcohol. The number of water molecules

consumed during accelerated ReaxFF hydrolysis in Bis A - JEFFAMINE D-230 is 11, whereas, in the Bis A - DETDA system, 14 water molecule is consumed at the end of the simulation. The higher consumption of water molecules and lower restrain energy in Bis A - JEFFAMINE D-230 can be related to a high rate of hydrolysis compared to Bis A - DETDA system. The diffusion of a water molecule to the C-O bond to participate in ether hydrolysis reaction might be impeded by a bulky aromatic ring of DETDA amine crosslinker in the Bis A - DETDA system. The **Figure 10C** illustrates the molecular weight reduction of the largest fragments in both epoxy thermosets during the hydrolysis reaction corroborates faster hydrolysis of the Bis A - JEFFAMINE D-230 than the Bis A - DETDA system. This can be due to the easy accessibility of water molecules to the vulnerable C-O bonds of ether linkages in the aliphatic amine cured epoxy network, whereas, the bulky aromatic rings in Bis A - DETDA system inhibit the mobility of water molecules to hydrolyzable C-O bonds in the ether linkages.

It is worth noting that the presented ReaxFF modeling framework can induce a paradigm shift in the modeling of destructive mechanisms of water-induced degradation in epoxy thermosets. In this study, we analyzed physical and chemical degradation in moist epoxy-amine thermosets separately. This modeling framework can be improved further in future studies by treating the physical and chemical degradation as a 'combined effect' in MD simulation to deconvolute the individual impact on hygrothermal degradation of the epoxy thermosets. We believe that the results of the current study will pave a way for future steps in investigating the hydrothermal degradation process using reactive forcefield, not only for epoxy thermosets but for other classes of crosslinked polymers as well.

4. CONCLUSIONS

In this study, the reactive force field (ReaxFF)-based molecular dynamics simulations are applied and used to provide the reactants with enough energy slightly larger than their lowest reaction barrier energy to overcome the barrier for crosslinking reaction. The ReaxFF method allows to build a realistic network at low temperature at a computationally accessible time scale and to avoid unwanted side reactions. This framework is implemented to crosslink the diglycidyl ether bisphenol-A (Bis A) with aliphatic amine (JEFFAMINE D -230) and aromatic amine (DETDA) to achieve a reasonably high crosslink percentage (70%). The effect of water absorption on thermomechanical properties of epoxy networks is systematically investigated. The interplay between free volume effects and hydrogen bonding interactions is analyzed for the decrease and recovery of elastic modulus in the epoxy networks. It is observed that water molecules tend to locate within the proximity of polar groups of epoxy networks and have a propensity to aggregate when exposed to higher water content. The ReaxFF framework is also utilized to investigate the chemical degradation of the crosslinked epoxy network. The JEFFAMINE D -230 cured epoxy network is found to be more susceptible to hydrolytic degradation than DETDA cured epoxy network. This lower hydrolytic degradation of DETDA cured epoxy polymers is accounted for in the inaccessibility of water molecules to interact with ether linkages in the DETDA cured epoxy network. Our results provide new insights to the reversible and irreversible hygrothermal aging process in the epoxy network and inform us about the new design criteria for broadening the application of epoxy materials, particularly in humid environments.

SUPPORTING INFORMATION

Force parameters examined for non-catalyzed reaction between epoxide and ammonia. Units for F_1 are kcal/mol and for F_2 are Å-2. Force parameters examined for non-catalyzed ether

hydrolysis reaction. Units for F₁ are kcal/mol and for F₂ are Å⁻². Detailed information on the epoxy-amine systems packed in the simulation box, assigning regions model for distinguishing reactive atoms during chemical reaction, crosslink conversion of Bis A- JEFFAMINE D-230 and Bis A-DETDA. Final structure of (B) *Bis A - JEFFAMINE D-230 (C) Bis A - DETDA*, The density vs time plot of Bis A- DETDA system with 5 wt.% of water content, Water interact with one hydroxyl group and H atom of the polymeric backbone to form TYPE II interactions, Log MSD log t plot vs MD simulation time for water molecules in the Bisphenol A epoxy-DETDA system at varying water contents at 600 K, The restrain energy plot against C-O reaction coordinates for hydrolysis of the Bis A -JEFFAMINE D-230 and Bis A -DETDA systems.

ACKNOWLEDGEMENTS

A.K., B.R. and W.X. acknowledge a support from the United States Navy's Office of Naval Research under grant number N00014-22-1-2129. A.K. acknowledges the support from Jessica Barnier (UW- Eau Claire) for proofreading and language editing of the manuscript. Authors acknowledge SCM (Software for Chemistry and Materials), Netherlands for providing license for ReaxFF module. Special thanks to Dr. Fedor Goumans and Dr. Ole Carstensen of SCM for their constant support. A.A. and W.X. acknowledge the support from the National Science Foundation (NSF) under NSF CMMI Award No. 2113558. This work is also supported in part by the NSF MRI Award OAC-2019077, ND EPSCoR Award #IIA-1355466 and by the State of North Dakota. Authors also thank the Extreme Science and Engineering Discovery Environment (XSEDE) for the award allocation (TG-DMR110088). Supercomputing support from CCAST HPC System at NDSU is acknowledged.

REFERENCES

- Yamini, S.; Young, R. J. The Mechanical Properties of Epoxy Resins. *J Mater Sci* 1980, *15* (7), 1823–1831. https://doi.org/10.1007/bf00550603.
- (2) Tran, P.; Wu, C.; Saleh, M.; Bortolan Neto, L.; Nguyen-Xuan, H.; Ferreira, A. J. M. Composite Structures Subjected to Underwater Explosive Loadings: A Comprehensive Review. *Compos Struct* 2021, 263 (August 2020), 113684. https://doi.org/10.1016/j.compstruct.2021.113684.
- Deyab, M. A.; Ouarsal, R.; Al-Sabagh, A. M.; Lachkar, M.; El Bali, B. Enhancement of (3) Corrosion Protection Performance of Epoxy Coating by Introducing New Hydrogenphosphate Compound. 2017, 107. Prog Org Coatings 37–42. https://doi.org/10.1016/j.porgcoat.2017.03.014.
- (4) Bolon, D. A. Epoxy Chemistry for Electrical Insulation. *IEEE Electr Insul Mag* **1995**, *11* (4), 10–18. https://doi.org/10.1109/57.400759.
- (5) Soutis, C. Fibre Reinforced Composites in Aircraft Construction. *Prog Aerosp Sci* 2005, *41* (2), 143–151. https://doi.org/10.1016/j.paerosci.2005.02.004.
- (6) VanLandingham, M. R.; Eduljee, R. F.; Gillespie, J. W. Moisture Diffusion in Epoxy Systems. J Appl Polym Sci 1999, 71 (5), 787–798. https://doi.org/10.1002/(SICI)1097-4628(19990131)71:5<787::AID-APP12>3.0.CO;2-A.
- (7) Xiao, G. Z.; Shanahan, M. E. R. Irreversible Effects of Hygrothermal Aging on DGEBA/DDA Epoxy Resin. *J Appl Polym Sci* **1998**, 69 (2), 363–369. https://doi.org/10.1002/(SICI)1097-4628(19980711)69:2<363::AID-APP18>3.0.CO;2-X.

- (8) Morel, E.; Bellenger, V.; Verdu, J. Structure-Water Absorption Relationships for Amine-Cured Epoxy Resins. *Polymer (Guildf)* **1985**, *26* (11), 1719–1724. https://doi.org/10.1016/0032-3861(85)90292-7.
- (9) Mohammadi, B.; Nokken, M. R. Influence of Moisture Content on Water Absorption in Concrete. *Proceedings, Annu Conf Can Soc Civ Eng* **2013**, *5* (January), 4092–4100.
- (10) Nasution, H.; Tantra, A.; Tommy Arista, P. The Effect of Filler Content and Particle Size on the Impact Strength and Water Absorption of Epoxy/Cockleshell Powder (Anadora Granosa) Composite. *ARPN J Eng Appl Sci* **2016**, *11* (7), 4739–4742.
- (11) Shen, M.; Almallahi, R.; Rizvi, Z.; Gonzalez-Martinez, E.; Yang, G.; Robertson, M. L. Accelerated Hydrolytic Degradation of Ester-Containing Biobased Epoxy Resins. *Polym Chem* **2019**, *10* (23), 3217–3229. https://doi.org/10.1039/c9py00240e.
- (12) Woo, R. S. C.; Chen, Y.; Zhu, H.; Li, J.; Kim, J. K.; Leung, C. K. Y. Environmental Degradation of Epoxy-Organoclay Nanocomposites Due to UV Exposure. Part I: Photo-Degradation. *Compos Sci Technol* 2007, 67 (15–16), 3448–3456. https://doi.org/10.1016/j.compscitech.2007.03.004.
- (13) Sharifi, M.; Ghorpade, K. A.; Raman, V. I.; Palmese, G. R. Synthesis and Swelling Behavior of Highly Porous Epoxy Polymers. *ACS Omega* **2020**, *5* (48), 31011–31018. https://doi.org/10.1021/acsomega.0c04035.
- (14) Cui, T.; Verberne, P.; Meguid, S. A. Characterization and Atomistic Modeling of the Effect of Water Absorption on the Mechanical Properties of Thermoset Polymers. *Acta Mech* **2018**, *229* (2), 745–761. https://doi.org/10.1007/s00707-017-1997-y.

- (15) Legghe, E.; Aragon, E.; Bélec, L.; Margaillan, A.; Melot, D. Correlation between Water Diffusion and Adhesion Loss: Study of an Epoxy Primer on Steel. *Prog Org Coatings* 2009, 66 (3), 276–280. https://doi.org/10.1016/j.porgcoat.2009.08.001.
- (16) Hamim, S. U.; Singh, R. P. Effect of Hygrothermal Aging on the Mechanical Properties of Fluorinated and Nonfluorinated Clay-Epoxy Nanocomposites. *Int Sch Res Not* **2014**, *2014*, 1–13. https://doi.org/10.1155/2014/489453.
- (17) Sharp, N.; Li, C.; Strachan, A.; Adams, D.; Pipes, R. B. Effects of Water on Epoxy Cure Kinetics and Glass Transition Temperature Utilizing Molecular Dynamics Simulations. *J Polym Sci Part B Polym Phys* 2017, 55 (15), 1150–1159. https://doi.org/10.1002/polb.24357.
- (18) Musto, P.; Ragosta, G.; Scarinzi, G.; Mascia, L. Probing the Molecular Interactions in the Diffusion of Water through Epoxy and Epoxy-Bismaleimide Networks. *J Polym Sci Part B Polym Phys* **2002**, *40* (10), 922–938. https://doi.org/10.1002/polb.10147.
- (19) Xiao, G. Z.; Delamar, M.; Shanahan, M. E. R. Irreversible Interactions between Water and DGEBA/DDA Epoxy Resin during Hygrothermal Aging. *J Appl Polym Sci* **1997**, *65* (3), 449–458. https://doi.org/10.1002/(sici)1097-4628(19970718)65:3<449::aid-app4>3.0.co;2-h.
- (20) Zhang, D.; Li, K.; Li, Y.; Sun, H.; Cheng, J.; Zhang, J. Characteristics of Water Absorption in Amine-Cured Epoxy Networks: A Molecular Simulation and Experimental Study. *Soft Matter* 2018, *14* (43), 8740–8749. https://doi.org/10.1039/c8sm01516c.
- (21) Hayward, D.; Hollins, E.; Johncock, P.; McEwan, I.; Pethrick, R. A.; Pollock, E. A. The Cure and Diffusion of Water in Halogen Containing Epoxy/Amine Thermosets. *Polymer*

- (Guildf) 1997, 38 (5), 1151–1168. https://doi.org/10.1016/S0032-3861(96)00614-3.
- Chen, M.; Jabeen, F.; Rasulev, B.; Ossowski, M.; Boudjouk, P. A Computational Structure—Property Relationship Study of Glass Transition Temperatures for a Diverse Set of Polymers. *J Polym Sci Part B Polym Phys* **2018**, *56* (11), 877–885. https://doi.org/10.1002/polb.24602.
- (23) Erickson, M. E.; Ngongang, M.; Rasulev, B. A Refractive Index Study of a Diverse Set of Polymeric Materials by QSPR with Quantum-Chemical and Additive Descriptors.

 *Molecules 2020, 25 (17), 1–9. https://doi.org/10.3390/molecules25173772.
- (24) Patnode, K.; Rasulev, B.; Voronov, A. Synergistic Behavior of Plant Proteins and Biobased Latexes in Bioplastic Food Packaging Materials: Experimental and Machine Learning Study. 2022. https://doi.org/10.1021/acsami.1c21650.
- (25) Jabeen, F.; Chen, M.; Rasulev, B.; Ossowski, M.; Boudjouk, P. Refractive Indices of Diverse Data Set of Polymers: A Computational QSPR Based Study. *Comput Mater Sci* 2017, 137, 215–224. https://doi.org/10.1016/j.commatsci.2017.05.022.
- (26) Okoli, C. P.; Adewuyi, G. O.; Zhang, Q.; Guo, Q. QSAR Aided Design and Development of Biopolymer-Based SPE Phase for Liquid Chromatographic Analysis of Polycyclic Aromatic Hydrocarbons in Environmental Water Samples. *RSC Adv* **2016**, *6* (75), 71596–71611. https://doi.org/10.1039/c6ra10932b.
- (27) Samantaray, P. K.; Little, A.; Wemyss, A. M.; Iacovidou, E.; Wan, C. Design and Control of Compostability in Synthetic Biopolyesters. **2021**. https://doi.org/10.1021/acssuschemeng.1c01424.

- (28) Khan, P. M.; Rasulev, B.; Roy, K. QSPR Modeling of the Refractive Index for Diverse Polymers Using 2D Descriptors. *ACS Omega* **2018**, *3* (10), 13374–13386. https://doi.org/10.1021/acsomega.8b01834.
- (29) Rasulev, B.; Jabeen, F.; Stafslien, S.; Chisholm, B. J.; Bahr, J.; Ossowski, M.; Boudjouk, P. Polymer Coating Materials and Their Fouling Release Activity: A Cheminformatics Approach to Predict Properties. ACS Appl Mater Interfaces 2017, 9 (2), 1781–1792. https://doi.org/10.1021/acsami.6b12766.
- (30) Patnode, K.; Demchuk, Z.; Johnson, S.; Voronov, A.; Rasulev, B. Computational Protein–Ligand Docking and Experimental Study of Bioplastic Films from Soybean Protein, Zein, and Natural Modifiers. *ACS Sustain Chem Eng* **2021**. https://doi.org/10.1021/acssuschemeng.1c01202.
- (31) Karuth, A.; Alesadi, A.; Xia, W.; Rasulev, B. Predicting Glass Transition of Amorphous Polymers by Application of Cheminformatics and Molecular Dynamics Simulations.

 *Polymer** (Guildf)** 2021, 218 (November 2020), 123495.

 https://doi.org/10.1016/j.polymer.2021.123495.
- (32) Varghese P. J, G.; Anna David, D.; Karuth, A.; Fatima Manamkeri Jafferali, J.; Begum P. M, S.; Jacob George, J.; Rasulev, B.; Raghavan, P. Experimental and Simulation Studies on Nonwoven Polypropylene–Nitrile Rubber Blend: Recycling of Medical Face Masks to an Engineering Product. ACS Omega 2022, 0 (0). https://doi.org/10.1021/acsomega.1c04913.
- (33) Clancy, T. C.; Frankland, S. J. V.; Hinkley, J. A.; Gates, T. S. Molecular Modeling for Calculation of Mechanical Properties of Epoxies with Moisture Ingress. *Polymer (Guildf)* **2009**, *50* (12), 2736–2742. https://doi.org/10.1016/j.polymer.2009.04.021.

- (34) Masoumi, S.; Valipour, H. Effects of Moisture Exposure on the Crosslinked Epoxy System:

 An Atomistic Study. *Model Simul Mater Sci Eng* **2016**, *24* (3).

 https://doi.org/10.1088/0965-0393/24/3/035011.
- (35) Lin, Y. C.; Chen, X. Investigation of Moisture Diffusion in Epoxy System: Experiments and Molecular Dynamics Simulations. *Chem Phys Lett* **2005**, *412* (4–6), 322–326. https://doi.org/10.1016/j.cplett.2005.07.022.
- (36) Wu, C.; Xu, W. Atomistic Simulation Study of Absorbed Water Influence on Structure and Properties of Crosslinked Epoxy Resin. *Polymer (Guildf)* **2007**, *48* (18), 5440–5448. https://doi.org/10.1016/j.polymer.2007.06.038.
- (37) Zhou, J. M.; Lucas, J. P. Hygrothermal Effects of Epoxy Resin. Part I: The Nature of Water in Epoxy. *Polymer (Guildf)* **1999**, *40* (20), 5505–5512.
- (38) Guha, R. D.; Idolor, O.; Grace, L. An Atomistic Simulation Study Investigating the Effect of Varying Network Structure and Polarity in a Moisture Contaminated Epoxy Network. *Comput Mater Sci* **2020**, *179* (January). https://doi.org/10.1016/j.commatsci.2020.109683.
- (39) Pandiyan, S.; Krajniak, J.; Samaey, G.; Roose, D.; Nies, E. A Molecular Dynamics Study of Water Transport inside an Epoxy Polymer Matrix. *Comput Mater Sci* **2015**, *106*, 29–37. https://doi.org/10.1016/j.commatsci.2015.04.032.
- (40) Lu, M. G.; Shim, M. J.; Kim, S. W. Effects of Moisture on Properties of Epoxy Molding Compounds. *J Appl Polym Sci* **2001**, *81* (9), 2253–2259. https://doi.org/10.1002/app.1664.
- (41) Science Arts & Métiers (SAM) Nonempirical Kinetic Modeling of Non-Fi Ckian Water Absorption Induced by a Chemical Reaction in Epoxy-Amine Networks Á Water

- Absorption Á Hydrolysis Á Fick 's Law. 2018.
- (42) Vashisth, A.; Ashraf, C.; Zhang, W.; Bakis, C. E.; Van Duin, A. C. T. Accelerated ReaxFF Simulations for Describing the Reactive Cross-Linking of Polymers. *J Phys Chem A* **2018**, *122* (32), 6633–6642. https://doi.org/10.1021/acs.jpca.8b03826.
- (43) Vashisth, A.; Ashraf, C.; Bakis, C. E.; van Duin, A. C. T. Effect of Chemical Structure on Thermo-Mechanical Properties of Epoxy Polymers: Comparison of Accelerated ReaxFF Simulations and Experiments. *Polymer (Guildf)* 2018, 158 (November), 354–363. https://doi.org/10.1016/j.polymer.2018.11.005.
- (44) Chenoweth, K.; Van Duin, A. C. T.; Goddard, W. A. ReaxFF Reactive Force Field for Molecular Dynamics Simulations of Hydrocarbon Oxidation. *J Phys Chem A* 2008, 112 (5), 1040–1053. https://doi.org/10.1021/jp709896w.
- (45) Chenoweth, K.; Cheung, S.; Van Duin, A. C. T.; Goddard, W. A.; Kober, E. M. Simulations on the Thermal Decomposition of a Poly(Dimethylsiloxane) Polymer Using the ReaxFF Reactive Force Field. *J Am Chem Soc* **2005**, *127* (19), 7192–7202. https://doi.org/10.1021/ja050980t.
- (46) Dasgupta, N.; Yilmaz, D. E.; Van Duin, A. Simulations of the Biodegradation of Citrate-Based Polymers for Artificial Scaffolds Using Accelerated Reactive Molecular Dynamics. *J Phys Chem B* **2020**, *124* (25), 5311–5322. https://doi.org/10.1021/acs.jpcb.0c03008.
- Valega Mackenzie, F. O.; Thijsse, B. J. Study of Metal/Epoxy Interfaces between Epoxy Precursors and Metal Surfaces Using a Newly Developed Reactive Force Field for Alumina
 Amine Adhesion. *J Phys Chem C* 2015, 119 (9), 4796–4804. https://doi.org/10.1021/jp5105328.

- (48) Polydore, C.; Roundhill, D. M.; Liu, H. Q. Nucleophile Assisted Hydrolysis of Carbon-Oxygen Bonds in Ethers. *J Mol Catal A Chem* **2002**, *186* (1–2), 65–68. https://doi.org/10.1016/S1381-1169(02)00138-3.
- (49) Liang, X.; Montoya, A.; Haynes, B. S. Molecular Dynamics Study of Acid-Catalyzed Hydrolysis of Dimethyl Ether in Aqueous Solution. *J Phys Chem B* **2011**, *115* (25), 8199–8206. https://doi.org/10.1021/jp201951a.
- (50) Senftle, T. P.; Hong, S.; Islam, M. M.; Kylasa, S. B.; Zheng, Y.; Shin, Y. K.; Junkermeier, C.; Engel-Herbert, R.; Janik, M. J.; Aktulga, H. M.; Verstraelen, T.; Grama, A.; Van Duin, A. C. T. The ReaxFF Reactive Force-Field: Development, Applications and Future Directions. *npj Comput Mater* 2016, 2 (September 2015). https://doi.org/10.1038/npjcompumats.2015.11.
- (51) Liu, L.; Liu, Y.; Zybin, S. V.; Sun, H.; Goddard, W. A. ReaxFF-Lg: Correction of the ReaxFF Reactive Force Field for London Dispersion, with Applications to the Equations of State for Energetic Materials. *J Phys Chem A* 2011, 115 (40), 11016–11022. https://doi.org/10.1021/jp201599t.
- (52) Zhang, W.; Van Duin, A. C. T. Improvement of the ReaxFF Description for Functionalized Hydrocarbon/Water Weak Interactions in the Condensed Phase. *J Phys Chem B* 2018, 122 (14), 4083–4092. https://doi.org/10.1021/acs.jpcb.8b01127.
- te Velde, G.; Bickelhaupt, F. M.; Baerends, E. J.; Fonseca Guerra, C.; van Gisbergen, S. J.
 A.; Snijders, J. G.; Ziegler, T. Chemistry with ADF. *J Comput Chem* 2001, 22 (9), 931–967. https://doi.org/10.1002/jcc.1056.
- (54) PLAMS, SCM, Theoretical Chemistry, Vrije Universiteit, Amsterdam, The Netherlands

- https://github.com/SCM-NV/PLAMS.
- (55) Bandyopadhyay, A.; Valavala, P. K.; Clancy, T. C.; Wise, K. E.; Odegard, G. M. Molecular Modeling of Crosslinked Epoxy Polymers: The Effect of Crosslink Density on Thermomechanical Properties. *Polymer (Guildf)* **2011**, *52* (11), 2445–2452. https://doi.org/10.1016/j.polymer.2011.03.052.
- (56) Fan, J.; Anastassiou, A.; Macosko, C. W.; Tadmor, E. B. Molecular Dynamics Predictions of Thermomechanical Properties of an Epoxy Thermosetting Polymer. *Polymer (Guildf)* 2020, 196 (December 2019), 122477. https://doi.org/10.1016/j.polymer.2020.122477.
- (57) Xin, D. R.; Han, Q. Molecular Dynamics Study on the Tensile Deformation of Cross-Linking Epoxy Resin. *J Mol Model* **2015**, *21* (1), 1–6. https://doi.org/10.1007/s00894-014-2567-z.
- (58) Brehm, M.; Thomas, M.; Gehrke, S.; Kirchner, B. TRAVIS—A Free Analyzer for Trajectories from Molecular Simulation. *J Chem Phys* **2020**, *152* (16). https://doi.org/10.1063/5.0005078.
- (59) Mortimer, S.; Ryan, A. J.; Stanford, J. L. Rheological Behavior and Gel-Point Determination for a Model Lewis Acid-Initiated Chain Growth Epoxy Resin.

 *Macromolecules** 2001, 34 (9), 2973–2980. https://doi.org/10.1021/ma001835x.
- (60) Anas, K.; David, S.; Babu, R. R.; Selvakumar, M.; Chattopadhyay, S. Energy Dissipation Characteristics of Crosslinks in Natural Rubber: An Assessment Using Low and High-Frequency Analyzer. *J Polym Eng* **2018**, *38* (8), 723–729. https://doi.org/10.1515/polyeng-2016-0425.

- (61) Atkins, P. The Elements of Physical Chemistry With Applications in Biology Chapter 16:
 Molecular Substances. 2001.
- (62) Papanicolaou, G. C.; Kosmidou, T. V.; Vatalis, A. S.; Delides, C. G. Water Absorption Mechanism and Some Anomalous Effects on the Mechanical and Viscoelastic Behavior of an Epoxy System. *J Appl Polym Sci* 2006, 99 (4), 1328–1339. https://doi.org/10.1002/app.22095.
- (63) Dannenberg, J. J. An Introduction to Hydrogen Bonding By George A. Jeffrey (University of Pittsburgh). Oxford University Press: New York and Oxford. 1997. Ix + 303 Pp. \$60.00. ISBN 0-19-509549-9. *Journal of the American Chemical Society* 1998, *120* (22), 5604–5604. https://doi.org/10.1021/ja9756331.
- (64) Popineau, S.; Rondeau-Mouro, C.; Sulpice-Gaillet, C.; Shanahan, M. E. R. Free/Bound Water Absorption in an Epoxy Adhesive. *Polymer (Guildf)* **2005**, *46* (24), 10733–10740. https://doi.org/10.1016/j.polymer.2005.09.008.
- (65) Tam, L. H.; Wu, C. Molecular Mechanics of the Moisture Effect on Epoxy/Carbon Nanotube Nanocomposites. *Nanomaterials* **2017**, 7 (10). https://doi.org/10.3390/nano7100324.
- (66) Yin, Q.; Zhang, L.; Jiang, B.; Yin, Q.; Du, K. Effect of Water in Amorphous Polyvinyl Formal: Insights from Molecular Dynamics Simulation. *J Mol Model* **2015**, *21* (1), 1–9. https://doi.org/10.1007/s00894-014-2551-7.
- (67) Vuković, F.; Walsh, T. R. Moisture Ingress at the Molecular Scale in Hygrothermal Aging of Fiber-Epoxy Interfaces. *ACS Appl Mater Interfaces* **2020**, *12* (49), 55278–55289. https://doi.org/10.1021/acsami.0c17027.

- (68) Capiel, G.; Uicich, J.; Fasce, D.; Montemartini, P. E. Diffusion and Hydrolysis Effects during Water Aging on an Epoxy-Anhydride System. *Polym Degrad Stab* **2018**, *153*, 165–171. https://doi.org/10.1016/j.polymdegradstab.2018.04.030.
- (69) Liu, T.; Guo, X.; Liu, W.; Hao, C.; Wang, L.; Hiscox, W. C.; Liu, C.; Jin, C.; Xin, J.; Zhang, J. Selective Cleavage of Ester Linkages of Anhydride-Cured Epoxy Using a Benign Method and Reuse of the Decomposed Polymer in New Epoxy Preparation. *Green Chem* 2017, 19 (18), 4364–4372. https://doi.org/10.1039/c7gc01737e.
- (70) El Yagoubi, J.; Lubineau, G.; Traidia, A.; Verdu, J. Monitoring and Simulations of Hydrolysis in Epoxy Matrix Composites during Hygrothermal Aging. *Compos Part A Appl Sci Manuf* **2015**, *68*, 184–192. https://doi.org/10.1016/j.compositesa.2014.10.002.